

## A Seismic Study of the Rift Zone in Northern Iceland

S.M. Zverev<sup>1</sup>, I.V. Litvinenko<sup>2</sup>, G. Pálmason<sup>3</sup>, G.A. Yaroshevskaya<sup>1</sup>, N.N. Osokin<sup>2</sup>, M.A. Akhmetjev<sup>4</sup>

<sup>1</sup> Institute of Physics of the Earth, USSR Academy of Sciences, B. Gruzinskaya 10, 123810 Moscow, USSR

<sup>2</sup> Mining Institute, 21 Line 2, 199026 Leningrad, USSR

<sup>3</sup> Orkustofnun, Grensásvegi 9, 108 Reykjavik, Iceland

<sup>4</sup> Geological Institute, USSR Academy of Sciences, Pyzhevsky St., 109017 Moscow, USSR

**Abstract.** The complex geological-geophysical expedition of the USSR Academy of Sciences jointly with the National Energy Authority (Orkustofnun) of Iceland conducted in 1977 a detailed seismic investigation of the flood basalt and rift zones in northern Iceland, similar to studies in southwestern Iceland. Continuous seismic profiling with 4–6 shot points was carried out across a total length of 90 km. In the flood basalt zone shallow refracting horizons were observed with  $V_p = 4.3\text{--}4.5$  km/s and tilted toward the rift zone. They closely correspond to dense sheets of flood basalts mapped geologically. Refracting and reflecting horizons at 2 to 12 or 15 km depth are tilted more gently in the same direction. A slight depression filled with neovolcanic formations with  $V_p < 3$  km/s exists near the surface in the rift zone. Reflectors with steep tilt can be traced to depths of 15 km. The deepest part of the depression is west of Mývatn in the region of current volcanism and rifting. A seismically homogeneous body without reflectors was detected under this region at 10–15 km depth. On the whole, the structure of the rift zone in northern Iceland is similar to, but more complex than, that of southwestern Iceland.

**Key words:** Iceland – Active rift zone – Neovolcanic zone – Crustal structure – Seismic profiling.

### Introduction

The complex geological-geophysical expedition of the USSR Academy of Sciences jointly with the National Energy Authority of Iceland conducted in 1976–1978 detailed seismic studies in various regions of Iceland; they were aimed at the problems of the origin and development of Iceland. In 1976 and 1977 the structural relationship of the modern rift zone with the adjacent flood basalts was studied. The inner structure of the flood basalts was studied in 1978. The results of the investigation of southwestern Iceland were published by Zverev et al. (1979; 1980). The present paper is the first publication of results obtained in northern Iceland.

### Location of Profile and Method of Observation

The investigations were conducted along a profile of about 90 km total length, using the road Akureyri-Mývatn-Grimstadir. The profile starts at Eyjafjörður in the west and runs eastward crossing the river Fnjóská and passing the lakes Ljósavatn, Mávratn, and Mývatn, and ends in the neovolcanic zone at the river Jökulsá á Fjöllum (Fig. 1). The profile crosses the main geological structures of northern Iceland: the flank of the Akureyri anticline, consi-

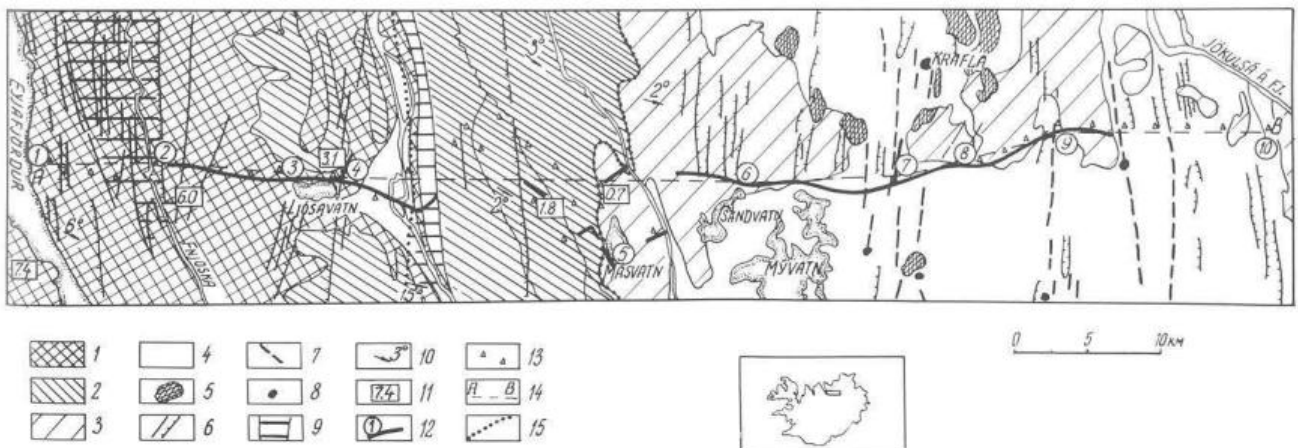


**Fig. 1.** Schematic geological map of the region under investigation. 1–4: volcanic formations of different ages; 1: Late Miocene-Pliocene (9 to 3 Ma); 2: Late Pliocene-Eopleistocene (3 to 0.7 Ma); 3: Pleistocene (<0.7 Ma); 4: Holocene; 5: dacite and rhyolite; 6: fissures; 7: fissures with Holocene volcanic activity; 8: main Late-Pleistocene and Holocene volcanic vents; 9: flexures; 10: direction and angle of tilt; 11: absolute age of volcanics in Ma; 12: seismic profile with numbers of shot points; 13: positions of automatic stations; 14: geological profile; 15: stratigraphic boundary

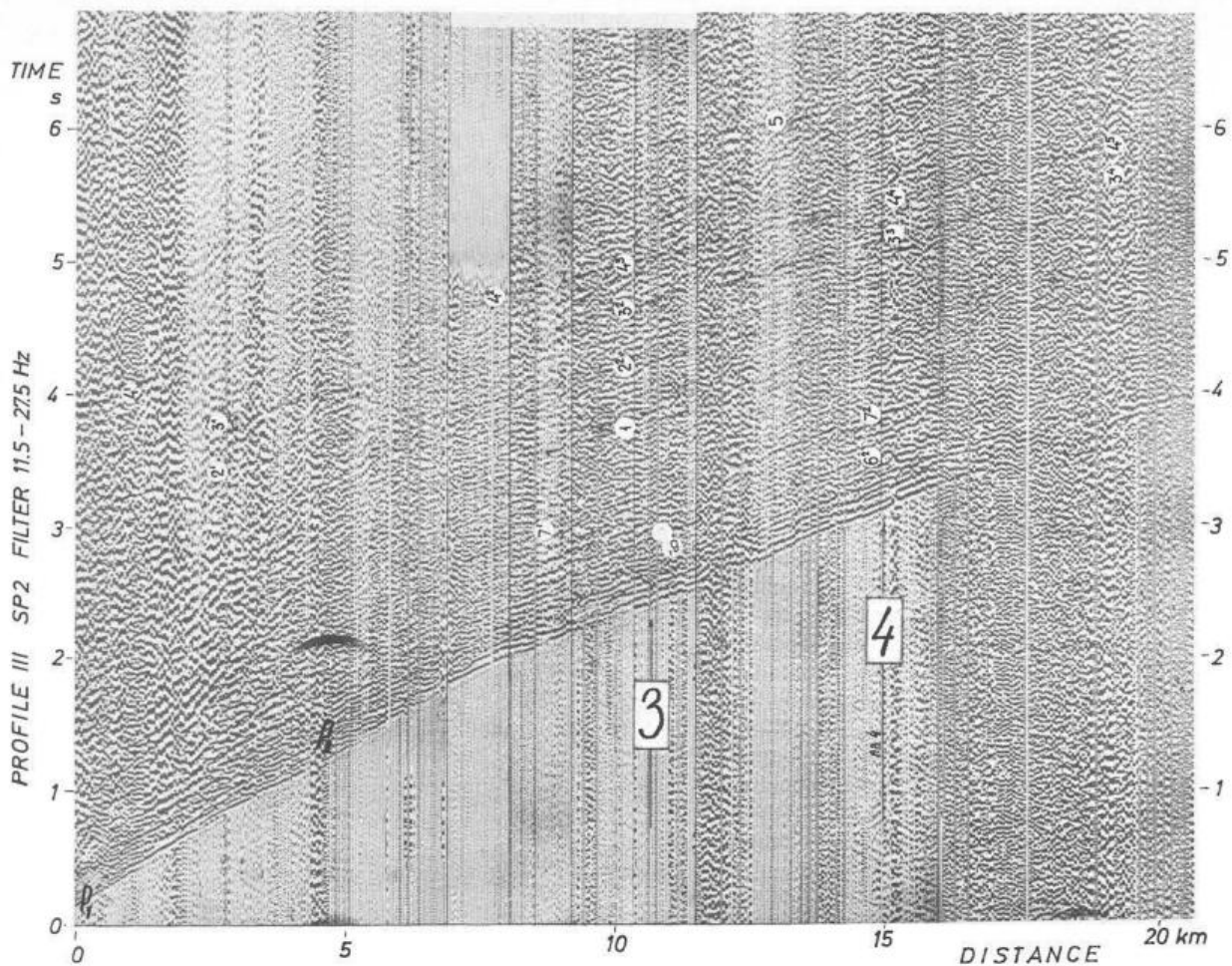


Fig. 2. The record section for SP2; frequency band 11.5–27.5 Hz; big numbers mark shot points, small numbers mark groups of reflected waves

sting of the flood basalt series, 8 or 9 to 3.1 Ma old (Pálmason and Saemundsson, 1974); an outer part of the neovolcanic zone with volcanic ages from 3.1 to 0.7 Ma; and the inner part of the neovolcanic zone with ages less than 0.7 Ma.

The method of observation was largely analogous to the one applied in southwestern Iceland in 1976 (Litvinenko, 1971; Zverev et al., 1979, 1980). On most of the profile continuous profiling was conducted with a multi-channel seismic system, except near Mývatn and Sandvatn where the road strongly deviates from the general profile direction. Here separate soundings were carried out with 2.3 km length each. A small gap in the observations east of Mývatn was caused by high background noise. Different from the work in southwestern Iceland, automatic three-component stations were used in addition to the multi-channel system, to fill the gaps of the continuous profiling and to extend the profile to the east and west (Fig. 1). This allowed us to construct piecewise-continuous travel-time curves for the first arrivals all along the profile.

Two 24-channel seismic refraction recording systems, SMOV-24, were used. The analogue magnetic tape records have a frequency band of 5 to 200 Hz and a dynamic range of 46 db. The geophones, SV-205, have a natural frequency of 5 Hz. Five geophones with a spacing of 50 m along the profile were connected to each channel; each group of geophones is 50 m from the next one; the length of the whole array is 2.3 km.

The automatic stations perform continuous magnetic tape recording in the frequency band of 2 to 30 Hz with a dynamic range of 46 db. Each station contains three-component geophones, SMN-KV, with a natural frequency of 0.5 Hz. The records of both types of instruments were played back on paper with the same band-pass filter setting. The multi-channel records were re-played with a variable-width script on the analogue system 'Ray'.

The shots were fired in a fjord (SP1), in rivers (SP2, 4, 7, 8, 10), in lakes (SP3, 5, 6), and in cavities of lava flows (SP9). The charges varied from several kilograms, when recording was near the shot points, to 120 kg and more, when recording was 40 to 60 km away. Charge sizes were chosen according to depth of water, the placing conditions, and the proximity to populated areas. The conditions at the shot influence the frequency content of the seismic waves (Burkhard and Vees, 1975); lower frequencies were activated by shots in shallow water and in lava cavities, higher frequencies by shots in deeper water. These peculiarities required careful adaptation of the frequency band during play-back.

#### Characteristics of the Seismic Wave Field

The wave field recorded on the northern profile is similar to the one observed in Southwest Iceland (Zverev et al., 1980) in terms

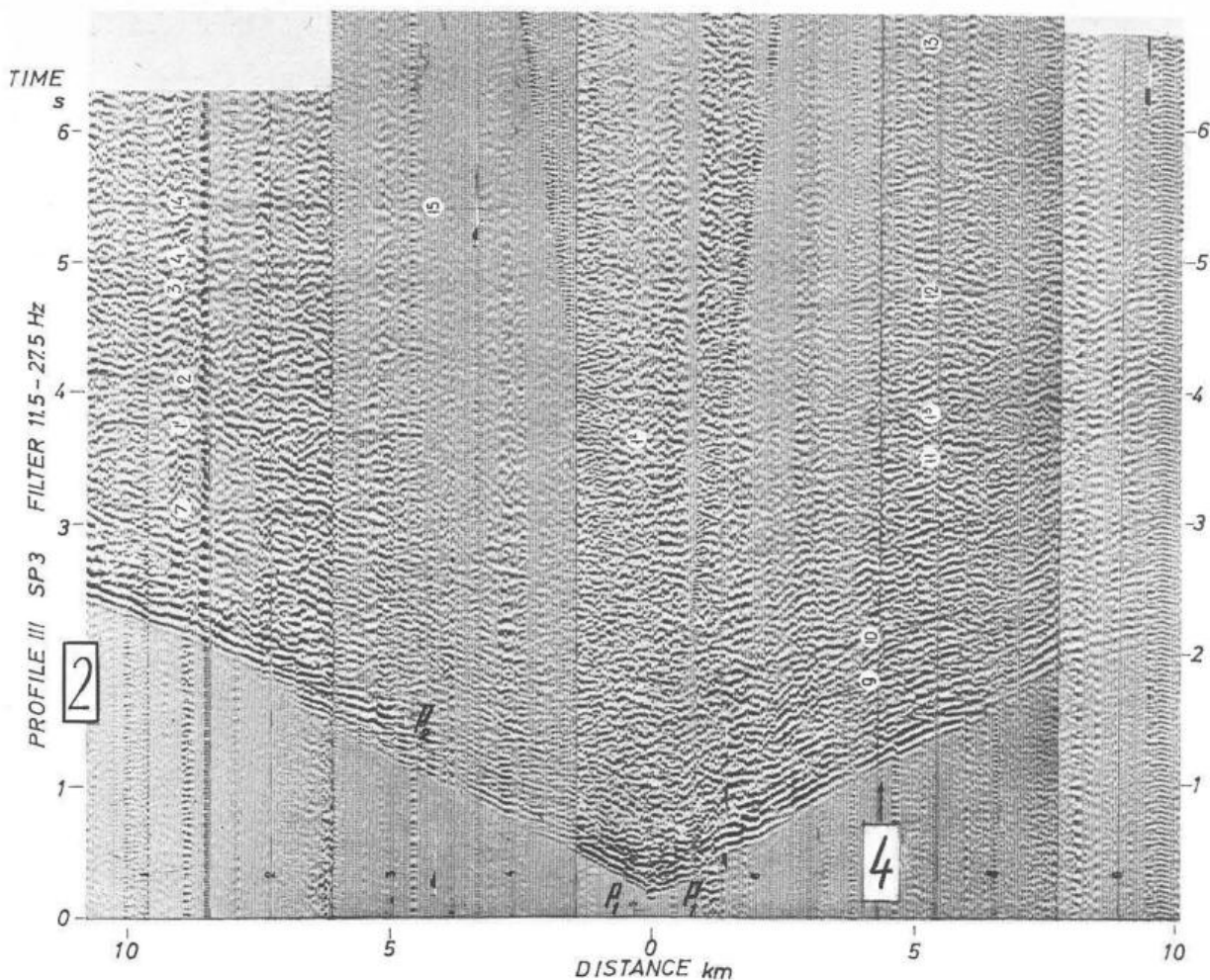


Fig. 3. Record section for SP3; for explanation see Fig. 2

of first-arrival travel-times, range of apparent velocities, characteristic wave forms, etc. Differences in the travel-time curves along the profiles involve more detail in the neovolcanic zone than in the flood basalt region, which might have resulted in data differences. It proved very advantageous that the transition zone could be filled with automatic stations and with isolated multi-channel soundings, because it revealed the nature of the cross-section in this zone.

The most important general features of the wave field are the following (Figs. 2-5):

1. A clear difference of the wave fields in the flood-basalt zone and in the neovolcanic zone both in range of velocities and in travel-times of first arrivals; asymmetry of refracted and reflected wave fields in the flood-basalt region, and symmetry in the neovolcanic zone.

2. In both zones the waves are connected with high-velocity sheets in the upper part of the lava series.

3. Absence of prominent reflections.

4. Considerable disturbances of the wave field by correlatable arrivals with high and even negative apparent velocities of uncertain origin, probably from near-surface faults.

It will be convenient to give a detailed description of the wave field separately for each wave type and each tectonic region.

### Characteristics of Refracted Wave Fields

In the flood-basalt region one can distinguish several groups of waves according to their kinematic and dynamic properties (Table 1). Low-velocity waves (1.6-1.8 km/s) are observed near shot points on low-velocity material; its thickness is 30-100 m. A monotonous increase of the apparent velocities with distance is rather typical for the travel-time branches of the  $P_1$  group mostly in the easterly direction (Figs. 2 and 6). These branches, more than 2-3 km long, have closely similar apparent velocities on overlap and attenuate at approximately the same locations. They probably represent waves propagating in high-velocity layers. No parallelism is observed at overlapping travel-time curves in the opposite direction. Waves of this group from various shot points have nearly the same travel-times. The minimum velocities near the shot points are 3.7-3.8 km/s. We interpret these observations to indicate that the flood basalt series is a gradient zone including high-velocity layers.

The change from group  $P_1$  to  $P_2$  in the travel-time diagram is rather clear (see e.g. SP2, Fig. 2). Outside the intersection region, these groups can be traced to the latest arrivals, but in short intervals only (1-2 km) because of disturbance from more intensive waves. The  $P_2$  group corresponds to a rather abrupt boundary.



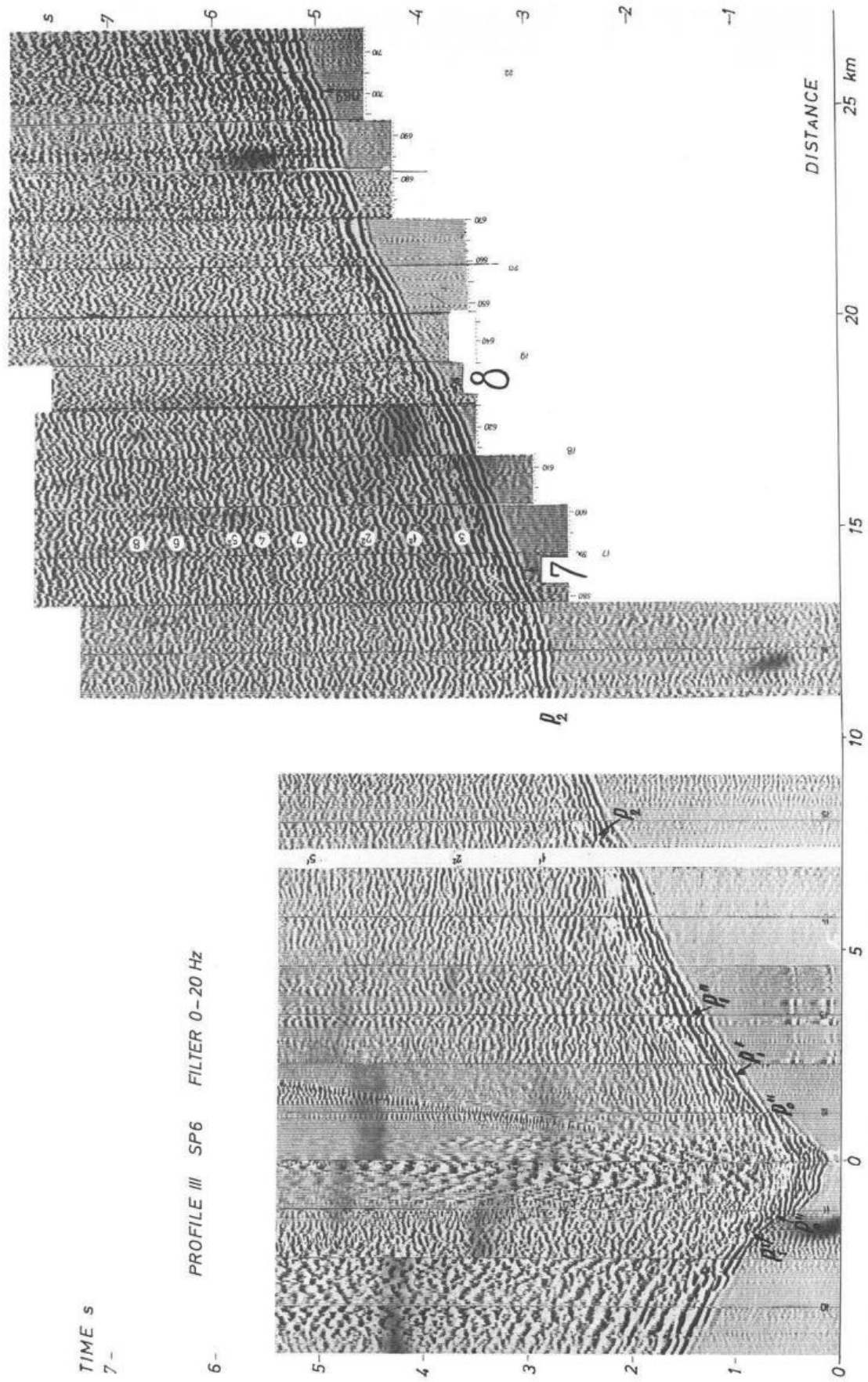


Fig. 4. Record section for SP6; frequency band: 0-20 Hz; for explanation see Fig. 2

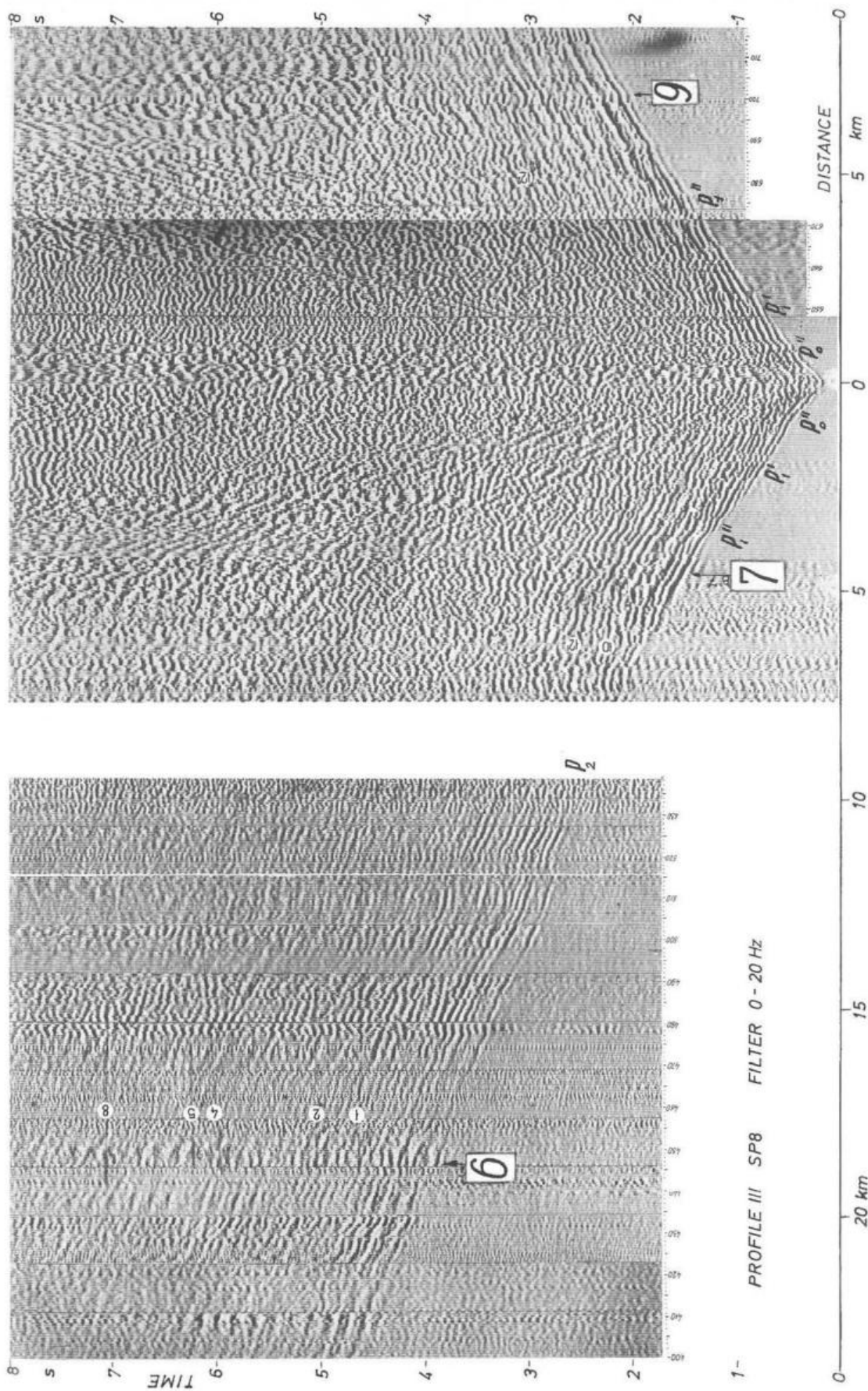


Fig. 5. Record section for SP8; frequency band: 0-20 Hz; for explanation see Fig. 2

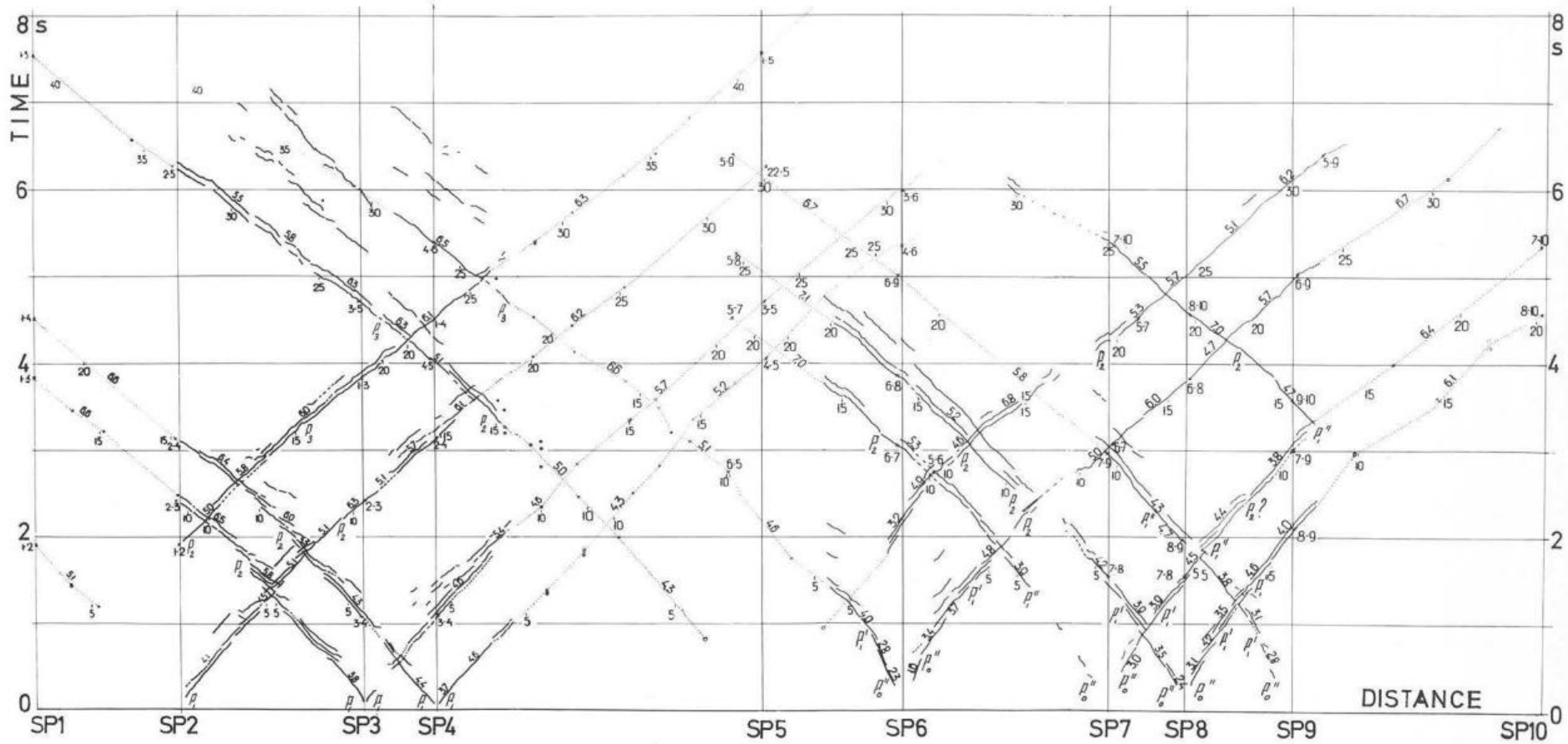


Fig. 6. Travel-time curves of refracted waves. The apparent velocities in km/s are marked at each branch

**Table 1.** Kinematic and dynamic properties of distinct wave groups

Index of group	$V^*$ (km/s) (average)	Intervals of tracing of the first arrivals (km)	$V$ (km/s) along the boundary	$\bar{V}$ (km/s) till the boundary	Comments
$P_1$	4.0–4.5	From 0 to 8–9	4.3–4.5	3.7–4	Till 2.5 km 4.0 km/s predominates, below: 4.5–4.7 km/s
$P_2$	5.5–6.0	To 15–16	5.6–5.7	4.4	
$P_3$	6.0–7.0	To 35	6.3–6.4	4.8	

**Table 2**

$P''_0$	2.8–3.5	From 0.5–1 to 1.5–2.5	3.2	1.9	Near SP $V=1.6$ – $2.0$ km/s
$P'_1$	3.9–4.0	To 4	4.0	2.3	
$P''_1$	4.2–4.8	To 8–10	4.5	3.2	
$P_2$	5.0–7.0	To 30	5.6–5.7	3.7	

The  $P_2$  group is the first arrival at distances from 8 or 10 to 15 km, while looking eastward the corresponding boundary is indicated to dip down; the increase in travel-times is remarkable. The travel-time curves in the only overlapping region (SP3–4 to the left, Fig. 2) demonstrate the existence of a slight velocity gradient in the layer. In contrast to Southwest Iceland, the  $P_2$  group need not be divided into two sub-groups. It is not clear whether this reflects peculiarities of structure or differences in observation.

The change from group  $P_2$  to  $P_3$  is less distinct.  $P_3$  is not clearly curved at greater distance, but it is possible to find a region of interference and a change in sign of the first arrivals. To the east the travel-times are greater than to the west for both groups. The waves are little attenuated and are supposed to be connected with a sharp velocity increase or a gradient zone with small steps.

In the neovolcanic zone the wave field distinctly differs from the one in the flood basalts in the following parameters (Figs. 4–6): (a) greater travel-times, (b) smaller velocities near the shot points, (c) symmetry in the travel-time curves east and west, (d) short segments of waves with  $V^*=4.5$  km/s, (e) longer segments of waves with  $V^*=6.0$  km/s, (f) absence of waves with  $V^*=6.3$ – $6.5$  km/s, as far as observed. The characteristics are summarized in Table 2.

In most cases waves of the  $P''_0$ ,  $P'_1$ , and  $P''_1$  groups have no reversed branches of the travel-time curves. They are identified at different shot points by their closely similar apparent velocities and travel-times at the same distances. They quickly attenuate and follow each other with time delays. They are considered to be waves transmitted through layers of constant high velocities within the lava series.

Waves of the  $P_2$  group begin to appear in later arrivals. They have a characteristic stable shape (Fig. 4) and are little attenuated. They can be clearly identified. They overlap in large regions (SP7–8 to the left, SP5–6 to the right). They are essentially parallel, which is surprising in view of their low attenuation.

In the eastern part of the profile (SP9, SP10) one can observe a change of the picture: a decrease of the travel-times and an increase of the recording range for the  $P_1$  group.

In the transition zone, the waves travelling through the flood basalts are seen at ranges smaller than 12 km on the records of the automatic stations (Fig. 7). Later waves arrive with 6.0 km/s and an increase of velocity is found at 18 km distance. The region of traceable waves through the flood basalts with 4.5 km/s is enlarged in the transition zone. Two groups,  $P_2$  and  $P_3$ , can be identified.  $P_2$  can be definitely traced through the flood basalts, the transition zone, and the neovolcanic zone by its intensity, velocity, and stability.

Amplitudes were determined on the basis of the records of the automatic stations to define regions with different attenuation. In the flood basalts attenuation is strong along the first few kilometers with  $\alpha_{\text{eff}}=4.6 \cdot 10^{-1} \text{ km}^{-1}$ , in the range of 8–30 km  $\alpha_{\text{eff}}=8 \cdot 10^{-2} \text{ km}^{-1}$ , and at greater distances the amplitudes are essentially constant.

A great number of phases with negative apparent velocities and merging with the first arrivals can be traced across distances of one to several kilometers (Figs. 2 and 3); their apparent velocities range from  $-3$  to  $-6$ , in rare cases to  $-10$  km/s. The phenomenon is enhanced in the higher frequencies.

### Peculiarities of the Reflections

Later arrivals are complex (Figs. 2–5). Low-velocity surface waves of 10–15 Hz can be seen to 2 or 3 km range. They can be suppressed by frequency filtering. Intensive sound waves make correlation of other waves at close range difficult. Many of the later arrivals are longitudinal reflected waves; also present are diffractions, shear waves, and converted waves. The longitudinal reflected waves among the later arrivals can be identified by their kinematic parameters: hyperbolic shape of the travel-time curve, interrelation of reversal and overlap times, etc. In intensity the reflections are usually lower than the first arrivals. Individual phases of the reflections can be traced for shorter distances (to several kilometers), but the groups can be traced across 10–15 km. Frequency filtering often enhances the reflected  $P$ -waves.

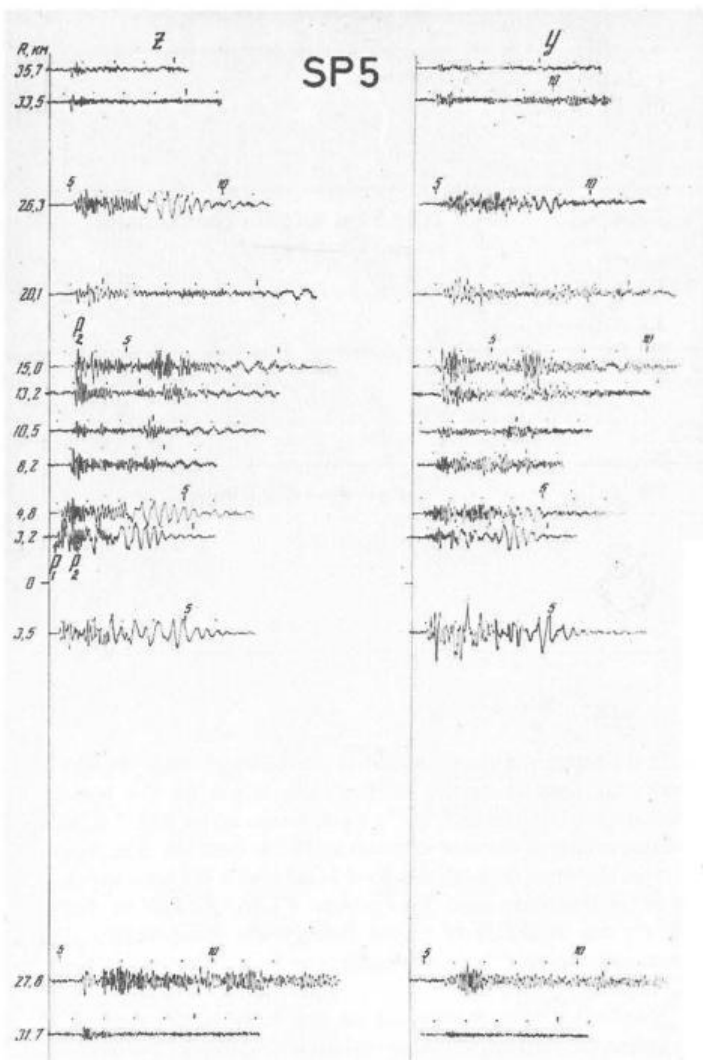


Fig. 7. Record section of automatic stations for SP5 in the frequency band of 5–18 Hz,  $V_{red}=6$  km/s

In the flood basalt region eight groups of reflected waves were found. The wave groups 1, 2, 3, 4, 7 (Figs. 2 and 3) are more clearly expressed than other waves, and all groups have reversed time curves. The former ones represent straight or slightly curved branches, 1–7 km long, from all three shot points, particularly from SP2 (Fig. 2). The later groups identified are numbered on Figs. 2 to 4. Their apparent velocities are greater than those of the first arrivals. Group 6 has a travel-time minimum clearly west of the shot point.

In the neovolcanic zone 12 groups of reflected waves were found on the basis of the reversed branches of the travel-time curves (Figs. 4 and 5). The branches are slightly curved with  $V^*=10$ –12 km/s extending to 15 km.

The ample occurrence of later phases which merge with the first arrivals and have positive or negative apparent velocities was already mentioned. Their travel-time branches are usually straight, sometimes hyperbolic. They are interpreted to be waves reflected from steeply dipping boundaries ( $>45^\circ$ ) and partly diffractions.

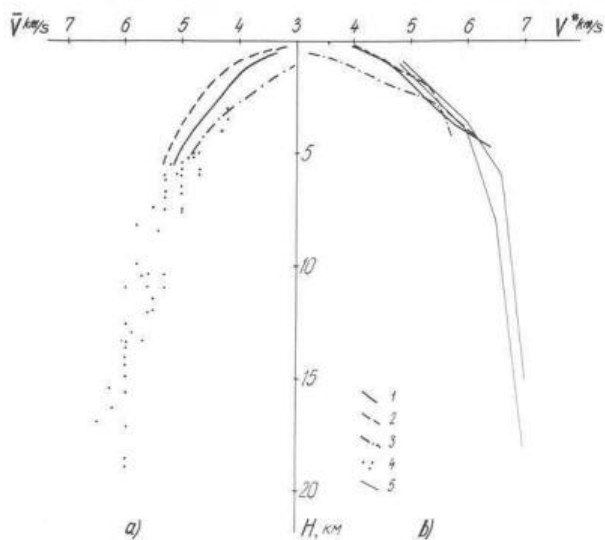


Fig. 8. Apparent (b) and average (a) velocities, computed from reflected (1–3) and refracted (4) waves. 1: flood basalts, SW-Iceland; 2: flood basalts, NE-Iceland; 3: neovolcanic zone, NE-Iceland; 5: apparent velocities computed from long-range refraction, NE-Iceland (RRISP Working Group, 1980)

### Seismic Cross-Sections

The average velocities used in the construction of the cross-section were determined from the refractions and the wide-angle reflections (Fig. 8a). A large scatter is observed for the reflections, and on average, they render lower velocities than the refractions. The apparent velocities which as the first approximation may be regarded as true layer velocities are shown as curve 2 in Fig. 8b; the corresponding velocities from Southwest Iceland (Zverev et al., 1980) are shown for comparison (curve 1). Curve 3 gives the velocities for the neovolcanic zone; they are considerably lower. For comparison, the results from a long-range refraction experiment are presented in curve 5 (RRISP Working Group, 1980; Gebrande et al., 1980). The seismic cross-section shown in Fig. 9 was derived from the refractions and reflections discussed above.

In the flood basalt region, from refraction data, inclined high-velocity layers were constructed from intercept times and apparent velocities with the assumption that group  $P_1$  is a head wave. Two boundaries were established with 4.3 and 4.5 km/s, respectively, and with  $8^\circ$  to  $10^\circ$  dip; the former continues eastward near-horizontally with 4.5 km/s as determined from SP3 and SP4 with the time-field method (Riznichenko, 1946). This method is based on drawing rays and isochrons for the seismic waves. It requires reversed and overlapping travel-time curves; there are no limitations concerning the velocity structure. A boundary with 5.75 km/s (between SP2 and SP3) and 5.65 km/s (between SP2 and SP4) was constructed with the time-field method from group  $P_2$ . The travel-time curves between SP1 and SP4 and between SP1 and SP3 give 5.6 km/s for this boundary. The computed depths were in good agreement. A third boundary with 6.3 km/s and  $5^\circ$  to  $7^\circ$  eastward dip was determined with the time-field method for SP1 to SP5.

In the neovolcanic zone, low-velocity refractions have no complete reversed branches in the travel-time curves. Average refractor velocities and intercept times were computed from all travel-time curves and depths were determined iteratively. However, the boun-



daries thus computed must be considered tentative, i.e. only generally representing the depth where the corresponding velocity is reached.

Group  $P_2$  has a travel-time curve to permit a time-field solution for SP6 and SP7 as well as for SP6 and SP8, giving closely similar depths for the 5.7 km/s boundary; it rises slightly towards the center of the neovolcanic zone. The lower boundary is shown approximately as the minimum depth of the velocity isoline of 6.3 km/s, constructed from the ends of the travel-time curves. The data from the automatic stations were used for the construction of velocity isolines only, and the numerical values of the velocities were chosen according to the boundary velocities.

Our cross-section (Fig. 9) is in good agreement with earlier seismic interpretations (Pálmason, 1971.) concerning the upper boundaries; there is some difference in depth and velocity below 2 km. The boundary depths with 5.1–6.8 km/s of Pálmason (1971) clearly depend on the length of the travel-time curves. Due to the detail of observation and to the reverse and overlapping travel-time curves, our section is considered very precise.

The refraction cross-section of the present northern profile (Fig. 9) is similar to the southwestern one (Zverev et al., 1980) in depths and in character of the boundaries in the flood basalt region, but the velocity values are lower in the north (5.7 and 6.3 km/s versus 6.0 and 6.5 km/s).

The construction of the cross-section from the reflections was done in several stages. First, groups of reflections with their vertices were used, nine in the flood basalt zone and 12 in the neovolcanic zone. The shorter reflecting elements were added. Dip vectors were constructed separately using square soundings. Average velocities were chosen such as to give the best agreement between the constructed boundaries. Figure 9 shows that the reflectors constructed from reflection vertices, one-sided branches, and dip vectors are in good agreement.

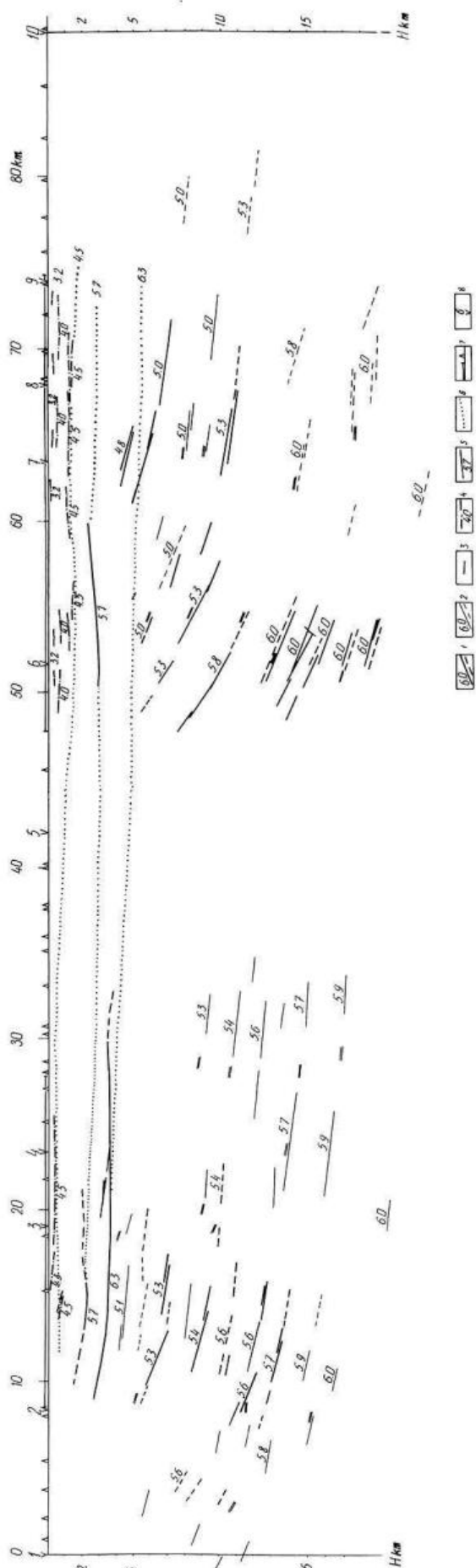
The reflectors form groups in certain depth intervals (<0.5 km), sometimes up to 5 or 7 km long. The greatest scatter of reflectors occurs at the ends of the profile outside the continuous observations.

On the western flank near SP2, the horizons dip  $15^\circ$ – $20^\circ$  eastward and less further east. This corresponds with the boundaries and velocity isolines from refraction. The steepest dips (up to  $40^\circ$ ) occur in the neovolcanic zone under SP6, shallowing again to the velocity contours in the neovolcanic zone.

## Discussion of the Results

Our seismic experiment gave more details than earlier work or that in southwestern Iceland (Zverev et al., 1980). Velocity contours, refractors, and reflectors were combined with geological

**Fig. 9.** Seismic cross-section. 1, 2: reflectors, computed from entire travel-time hyperbola (1) or from isolated branches (2); *dashed lines* less reliable; *numbers* indicate average velocities *above* reflectors. 3: Dip of reflectors. 4: Refractors coinciding with geological boundaries. 5: Refractors computed from reversed travel-time curves; *dash-dotted*: from unreversed lines; *numbers* indicate refractor velocities. 6: Velocity contours: 4.5, 5.7, 6.3 km/s. 7: regions of multi-channel coverage and projected positions of automatic stations (Fig. 1). 8: Shot points



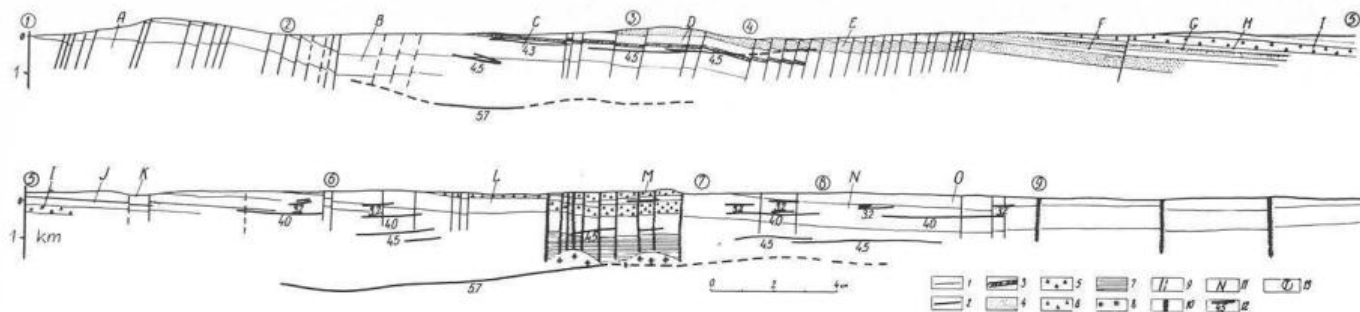


**Fig. 10.** Geological cross-sections combined with seismic results. 1: lithostratigraphic boundaries; 2: stratigraphic boundaries (3.1 and 0.7 Ma); 3: basalt; 4: basalt alternating with tuffaceous sediments; 5: pyroclastic and glacio-fluviatile formations; 6: agglomerates, volcanic breccias, tuffs; 7: dolerite, gabbro; 8: granophyre; 9: faults; 10: zones of recent volcanism; 11: indices of main subdivisions of the cross-section:

*Upper Miocene – Lower Pliocene.* A: Porphyrites, olivine basalt, etc.; B: aphyric basalt; C: aphyric and fine-grained porphyric basalt, porphyrite, dolerite; D: basalt, porphyrite, icelandite, tuff, tuffaceous sediments; E: basalt, andesite-basalt, series of tuffaceous sediments in top and bottom of layers; F: basalt, agglomerate, tuff.

*Upper Pliocene – Eopleistocene.* G: Tillite, tuffaceous sediments of glacio-fluviatile origin, hyaloclastite; H: olivine basalt; I: hyaloclastite, tillite; J: basalt.

*Pleistocene.* K, L: Basalt, tillite; M: agglomerate, lava breccia, tuff; N: basalt, tillite; O: late Pliocene and Holocene lava. 12: refractors and corresponding velocities; 13: shot points

observations and published data. The results are a schematic geological map (Fig. 1) and a geological cross-section along the seismic profile (Fig. 10).

Separate seismic waves arise at sharp or gradual changes of physical rock properties. Refractions are generated at velocity increases with depth which may occur in bulk or in thin layers. Reflections originate at discontinuities of acoustic impedance with increasing or decreasing velocities. Reflecting horizons may correspond to contact zones of rocks of different composition or metamorphic grade and to faults, dykes, etc.

The seismic profile crosses the main geological structures of northern Iceland (Fig. 1). The total thickness of the exposed section is estimated 4 000 m. The lower part of the rocks older than 3.1 Ma is 2 500–3 000 m thick and consists predominantly of lava. East of SP3 only one layer of tuffaceous sediments is observed which thickens to the east. In the outer and inner neovolcanic zone the rocks are in almost equal amounts lava, pyroclastites, and tuffaceous sediments mostly of fluvio-glacial origin. Separate series probably have different seismic velocities.

The strip along the profile can be divided into five tectonic regions (Fig. 1). The western-most region includes the eastern slope of the water divide between Eyjafjörður and the river Fnjóská (SP1–2); it is characterized by a monocline composed of flood basalts (Fig. 10) dipping increasingly  $5^{\circ}$ – $6^{\circ}$  to  $20^{\circ}$ – $30^{\circ}$ . The flexure is accompanied by faults, dykes, and a narrow graben in which the flood basalts have maintained their original flat bedding. The second region between Fnjóská and Skjálfafljót (SP2–4) is characterized by flat bedding ( $3^{\circ}$ – $5^{\circ}$  dip) and comparatively rare faults and dykes of northeasterly trend. In the adjoining third region to 7 km east of SP4 there are many faults and dykes of northerly trend. The total throw of the faults from the Akureyri anticline to the edge of the neovolcanic zone is not less than 100–150 m and increases from south to north. The fourth region is also characterized by flat bedding with minor faults and dykes and an increasing proportion of fluvio-glacial formations including large series of pillow lavas, hyaloclastites, and tillites. The fifth region is the inner neovolcanic zone largely built of Pleistocene and Holocene volcanics. Four centers of modern volcanism can be identi-

fied: Krafla, Búrfell, Rauduborgir, and Nýjahraun (Figs. 1 and 10). The latter two are crossed by the profile in the east.

On the cross-sections (Figs. 9 and 10) we note the good agreement in the flood basalt zone (the above regions 1 to 3) between the seismic refractors and the geological boundaries near the surface. Near SP3 the 4.3–4.5 km/s horizons exactly coincide with dense basalts (layers C and D, Fig. 10). Near SP4 the 4.5 km/s horizon corresponds to the base of layer E with a large content of low-velocity tuffaceous sediments. West of SP3 (Fig. 9) the 4.3–4.5 km/s refractors do not agree with the shape of the velocity contours; the refractors are dense basalt layers while the velocity contours represent the general velocity increase. Commonly in the flood basalt zone, the refractors parallel the velocity contours and the refractors to great depth as they parallel the shallow geological boundaries. This suggests a long history of invariable flood basalt deposition. Hence the age of the rocks (3 Ma for the 4 000 m exposed section) is expected to increase with depth.

The rift zone is more complicated. The refractors and the 4.5 km/s contour are depressed west of SP7, i.e., east of Mývatn. A second depression occurs east of SP8. These two depressions consist of low-velocity rocks (3.2 and 4.0 km/s refractors). All the above refractors coincide or are parallel to the geological boundaries. The 5.7 km/s contour is slightly arched, culminating at 2.5 km depth under Námafjall on the Krafla fissure swarm (Saemundsson, 1974; 1977; 1978) which currently experiences a rifting episode (Björnsson et al., 1977; 1979; several papers, this volume).

The deeper reflectors in the neovolcanic zone distinctly intersect the refractors. Maximum reflector slopes are  $30^{\circ}$ – $40^{\circ}$  (under SP6) decreasing eastward. Two zones with conspicuous absence of deep reflectors occur west of SP7 under the axial depression and under SP9 where the surface layers are also depressed (Figs. 1 and 10). Both are characterized by active fissure swarms. It is suggested that the absence of reflectors is evidence for magma chambers.

The seismic cross-sections in northeastern and southwestern Iceland are very similar. In the flood basalts the near-surface seismic horizons closely correspond to geological layers. Both we-

stern flanks are complex with ancient flexures at Borgarfjörður and Fnjóská, respectively. Near the neovolcanic zones the whole basalt series is slightly tilted toward their centers. The depressions in the neovolcanic zones are filled with low-velocity rocks. Steep dip angles are found to depths of 15 km and more. At the centers of the depression there are active volcanic fissure swarms, below which, at 10–15 km depth, there is evidence for seismically homogeneous bodies which are interpreted to be magma chambers. On the whole the northeastern zone is more complex than the southwestern one.

The spatial continuity of structure from 10–15 km depth to the surface activity of volcanism and rifting is considered by some of the authors to be evidence for temporal continuity of structure and for stability without significant spreading in Iceland. In this view the recent activity is superimposed on ancient crustal structure. Others believe that the spatial continuity indicates a steady-state process (in a time-average sense) of spreading, rifting, and generation of new lithosphere where, however, complications in structure may have arisen from a shifting of the active zone from one location to another.

*Acknowledgements.* The seismic studies in northern Iceland were carried out in 1977 by the Soviet Geodynamic Expedition of the USSR Academy of Sciences, jointly with the Geothermal Division of the National Energy Authority of Iceland. Great help in the seismic work was rendered by Corresponding Member of the USSR Academy of Sciences, Professor V V Belousov. Beside the authors, the following Soviet scientists participated in the seismic field work. G.N. Akimov, A.N. Fursov, V V Knjasev, B.I. Kerby, O.A. Kisilev, N.M. Nardov, E.M. Chesnokov (Institute of Physics of the Earth of the USSR Academy of Sciences); Yu.M. Misnik, N.V. Kondratjev, A.V. Konoplev, V.I. Gatiev (Leningrad Mining Institute); and in geological mapping: A.R. Geptner (Geological Institute, USSR Academy of Sciences). S. Sigurmundsson, G. Petursson, and G. Stefansson were instrumental for the field work. The results were discussed with K. Saemundsson. The Embassy of the USSR in Iceland and the National Research Council of Iceland helped much in the organization of the Expedition's work. We are grateful to all of them.

## References

- Björnsson, A., Johnsen, G., Sigurdsson, S., Thorbergsson, G., Tryggvason, E.: Rifting of the plate boundary in North Iceland 1975–1978. *J. Geophys. Res.* **84**, 3029–3038, 1979
- Björnsson, A., Saemundsson, K., Einarsson, P., Tryggvason, E., Grönvold, K.: Current rifting episode in North Iceland. *Nature* **266**, 318–323, 1977
- Burkhardt, H., Vees, R.: Explosions in shallow water for deep seismic sounding experiments. *J. Geophys.* **41**, 463–474, 1975
- Gebrande, H., Miller, H., Einarsson, P.: Seismic structure of Iceland along RRISP Profile I. *J. Geophys.* **47**, 239–249, 1980
- Litvinenko, I.V.: Seismic methods of studying the complex structure of the upper part of the continental crust. *Notes Leningrad Mining Inst. V XI (2)*, 1971
- Pálmason, G.: Crustal structure of Iceland from explosion seismology. *Soc. Sci. Isl.* **40**, 187pp., 1971
- Pálmason, G., Saemundsson, K.: Iceland in relation to the Mid-Atlantic Ridge. *Annu. Rev. Earth. Planet. Sci.* **2**, 25–50, 1974
- RRISP Working Group: First results from the Reykjanes Ridge Iceland Seismic Project 1977. *Nature* **279**, 56–60, 1979
- RRISP Working Group: Reykjanes Ridge Iceland seismic experiment (RRISP 77). *J. Geophys.* **47**, 228–238, 1980
- Riznichenko, Yu.V.: Geometrical seismology of stratified media (in Russian). *Proc. Inst. Theor. Geophys.* **II**, 1946
- Saemundsson, K.: Evolution of the axial rifting zone in northern Iceland and the Tjörnes fracture zone. *Bull. Geol. Soc. Am.* **85**, 495–504, 1974
- Saemundsson, K.: Geological Map of Iceland, Sheet 7. Reykjavik, Mus. Nat. Hist., 1977
- Saemundsson, K.: Fissure swarms and central volcanoes of the neovolcanic zones of Iceland. *Geol. J. Spec. Iss.* **10**, 415–432, 1978
- Zverev, S.M., Litvinenko, I.V., Pálmason, G., Yaroshevskaya, G.A., Osokin, N.N.: A seismic study of the western rift in southern Iceland (in Russian). *Bull. Mosk. O-va ispit. priropi. otd. geol. (Bull. MOIP)*, Vol. 54, No. 3, 1979
- Zverev, S.M., Litvinenko, L.V., Pálmason, G., Yaroshevskaya, G.A., Osokin, N.N.: A seismic crustal study of the axial rift zone in southwest Iceland. *J. Geophys.* **47**, 202–210, 1980

Received June 20, 1979; Revised Version August 20, 1979